Predictive Control and Estimation Algorithms for the NASA/JPL 70-Meter Antennas

W. Gawronski
Ground Antennas and Facilities Engineering Section

This article presents a modified output-prediction procedure and a new controller design based on the predictive control law. Also, a new predictive estimator is developed to complement the controller and to enhance system performance. The predictive controller is designed and applied to the tracking control of the Deep Space Network 70-m antennas. Simulation results show significant improvement in tracking performance over the linear-quadratic controller and estimator presently in use.

I. Introduction

The recent pointing requirements for the X-band (8.4 GHz) frequency, 70-m aperture antenna (further denoted as the DSS 14 antenna) and the expectation of future K-band (32 GHz) capability dictate a need for high-performance controllers for the azimuth and elevation drives. This article presents a new design procedure for a tracking controller that significantly improves antenna tracking performance. It considers on-axis (or servo) tracking. In this case, the output is taken on the encoder (or tachometer) rather than the radio frequency (rf) pointing position. The predictive controller uses future values of the stored input command to generate the control signal. For this reason, the predictive control principle is considered useful in design of the Deep Space Network (DSN) antennas' tracking controllers, since the antenna future tracking command is known when following stars or spacecraft.

The tracking-control problem is a nontrivial extension of the regulator problem, widely investigated in the control literature. Several approaches to the solution of the tracking problem have been presented in [1–11]. Predictive controllers are described and analyzed in many papers, among them [1,4,5,6,7,9,10,11]. In most of them, controlled auto-regressive and integrated moving-average (CARIMA) models are developed and extensively used for output prediction and predictive control of linear systems [1,4,5,6,7,9,10]. State-space description serves as a standard tool for system analysis and design. Besides tool standardization, the state-space representation of a predictive control system provides a unique insight into system properties, improves system design, and simplifies analysis. Interpretations of CARIMA modeling in the state space are provided by [1,4,11].

This article presents a state-space description of the output-prediction procedure and a new controller design based on the predictive control law. A new input-reference scheme that uses the input-reference horizon is introduced. Thus, the increment of the control signal is determined with respect to the input horizon rather than to the last

value of the input. Also, the introduced weighting matrix includes a forgetting factor. Both features significantly improve system performance.

The usefulness of the predictive control law depends on the availability of the plant-state variables for measurement. Typically, not all state variables can be measured, although for an observable system they can be estimated. In this article, a predictive estimator is developed as a complement to the predictive controller to speed the estimation process and enhance system performance.

Using the introduced predictive control and estimation laws, the state-space predictive controller is designed and applied to the tracking control of the DSN 70-m antennas. Simulation results show significant improvement in tracking performance over the linear-quadratic (LQ) controller and estimator presently in use. The robustness to parameter variation and the disturbance-suppression properties are found to be fairly good for the considered predictive control system.

II. Output Prediction for a Linear System

A plant with nu inputs and ny outputs is considered. Its linear state-space model consists of n states

$$x(i+1) = Ax(i) + Bu(i), \quad y(i) = Cx(i) + Du(i) \tag{1}$$

where $x \in R^n$, $u \in R^{nu}$, and $y \in R^{ny}$. The task is to predict output y for NY steps ahead, given projected input u for NU steps ahead. The integer NY is the length of the output horizon, while NU is the length of the input horizon. For casual systems, the length of the input horizon does not exceed the length of the output horizon, i.e., $NU \leq NY$.

Before determining the predicted output, the input and output sequences (or horizons) are introduced. Three types of input sequences are defined. First is the input horizon $U(i)$, consisting of the input from an instant i up to $NU - 1$ steps ahead

$$U^T(i) = [u_i^T(0), u_i^T(1), \ldots, u_i^T(NU-1)] \tag{2}$$

where $u_i(k)$ is the predicted input at instant i with k steps ahead. The input horizon $U(i-1)$ is a horizon predicted at the previous time instant. Note that it is not a delayed prediction at instant i, i.e., $u_{i-1}(k) \neq u_i(k-1)$.

The second sequence, reference-input horizon $U_r(i)$, is identical to the previous input horizon $U(i-1)$ for the first NR time instants and is constant for the remaining $NU - NR$ instants

$$u_r(k) = \begin{cases} u_{i-1}(k) & \text{for } k = 1, \ldots, NR \\ u_{i-1}(NR) & \text{for } k = NR+1, \ldots, NU \end{cases} \tag{3}$$

where the integer $NR \leq NU$ is the length of the reference horizon. Thus,

$$U_r(i) = EU(i-1) \tag{4}$$

where

$$E = \begin{bmatrix} E_1 & 0 \\ E_2 & 0 \end{bmatrix}, \quad \underbrace{E_1 = \text{diag}(I_{nu}, \ldots, I_{nu})}_{NR \text{ times}}$$
$$E_2 = \begin{bmatrix} 0 & I_{nu} \\ \vdots & \vdots \\ 0 & I_{nu} \end{bmatrix} \Big\} NR \text{ times} \tag{5}$$

and I_{nu} is the identity matrix of dimension nu.

The last input sequence, input-increment horizon $\Delta U(i)$, is defined with respect to reference horizon $U_r(i)$ as follows:

$$\Delta U(i) = U(i) - U_r(i) = U(i) - EU(i-1) \tag{6}$$

Sequences $U(i)$, $U(i-1)$, $U_r(i)$, and $\Delta U(i)$ are shown in Fig. 1.

Two output sequences are introduced: output horizon Y

$$Y(i)^T = [y_i^T(1), y_i^T(2), \ldots, y_i^T(NY)] \tag{7}$$

and predicted-output horizon $\overline{Y}$

$$\overline{Y}^T(i) = [\overline{y}_i^T(1), \overline{y}_i^T(2), \ldots, \overline{y}_i^T(NY)] \tag{8}$$

The latter is an output of the system with reference horizon U_r as an input. Components $y_i(k)$ and $\overline{y}_i(k)$ are the output and predicted output, respectively, at instant i with k steps ahead. Note that although the system output at instant i with k steps ahead is equal to the output at instant

$i+l$ with $k-l$ steps ahead, $y_i(k) = y_{i+1}(k-l) = y(i+l)$, $l < k$, the same is not true for the predicted output. The prediction at instant i with k steps ahead is not the same as the prediction at instant $i+l$ with $k-l$ steps ahead.

The output horizon is obtained from the plant model, Eq. (1), for $k = 1, \ldots, NY$:

$$y(i+k) = CA^k x(i) + CA^{k-1}Bu(i) + \ldots + CBu(i+k-1) \quad (9)$$

Predicted output $\overline{y}_i(k)$ is defined as a system response to the reference-horizon input $U_r(i)$. Thus, for $k = 1, \ldots, NY$

$$\overline{y}_i(k) = CA^k x(i) + CA^{k-1}Bu_r(1) + \ldots + CBu_r(k) \quad (10)$$

and Eq. (9) is now

$$y(i+k) = \overline{y}(k) + CA^{k-1}B\Delta u_i(0) + \ldots + (CA^{k-NR-1}B + \ldots + CB)\Delta u_i(NR-1) \quad (11)$$

Denoting the Markovian matrix

$$G = \begin{bmatrix} g_1 & 0 & \ldots & 0 \\ g_2 & g_1 & \ldots & 0 \\ \ldots & \ldots & \ldots & \ldots \\ \ldots & \ldots & \ldots & \ldots \\ g_{NU} & g_{NU-1} & \ldots & g_1 \\ \ldots & \ldots & \ldots & \ldots \\ g_{NY} & g_{NY-1} & \ldots & g_{NY-NU+1} \end{bmatrix} \quad (12)$$

where $g_i = CA^{i-1}B$ is the ith Markov parameter, one obtains the output horizon from Eq. (11):

$$Y(i) = \overline{Y}(i) + G\Delta U(i) \quad (13)$$

Predicted-output horizon $\overline{Y}$, necessary to determine Y in Eq. (13), is determined from Eq. (10):

$$\overline{Y}(i) = Hx(i) + GU_r(i) = Hx(i) + GEU(i-1) = Hx(i) + FU(i-1) \quad (14)$$

where

$$F = GE, \quad H = \mathcal{O}_{NY-1}A \quad (15)$$

E is as given by Eq. (5), and

$$\mathcal{O}_{NY-1} = [C^T(CA)^T \ldots (CA^{NY-1})^T]^T \quad (16)$$

The input-increment horizon depends on the length of the reference horizon. In particular, for $NR = 1$, one obtains $\Delta u_i(k) = u_i(k) - u_{i-1}(1)$, $k = 1, \ldots, NU$. This is the case of the generalized predictive control of [5], where the control increments are defined with respect to the last input command. For $NR = NU$, one obtains $E = I$ and $\Delta U(i) = U(i) - U(i-1)$. In this case, the control increment is defined with respect to the previous control over the whole length of the input horizon. If the input increment is determined with respect to the zero-reference input, the input-increment horizon is equal to the input horizon, $\Delta U(i) = U(i)$, and for this case, $NR = 0$. Signal sequences $U(i)$, $U(i-1)$, $U_r(i)$, and $\Delta U(i)$ are shown in Fig. 1 for $NR = 0$, 1, and NU and for a generic NR. Note also that for $NR = NU$ one obtains $F = G$, for $NR = 1$ one obtains $F^T = [g_1^T, g_1^T + g_1^T, \ldots, g_1^T + \ldots + g_{NY}^T]$, and for $NR = 0$ one obtains $F = 0$. In the latter case, the output is predicted from the system state only, while otherwise it is predicted from the state and the system input as well.

III. Predictive Control

The basic task for a predictive controller is to assure that for the bounded input the future output Y will closely follow the input command Y_o within the output horizon NY:

$$Y_o^T(i) = [y_{oi}^T(1), y_{oi}^T(2), \ldots, y_{oi}^T(NY)] \quad (17)$$

where $y_{oi}(k)$ is the command signal at instant i with k steps ahead. Thus, the task is to minimize the plant tracking error while the input remains bounded:

$$\varepsilon(i) = Y_o(i) - Y(i) \quad (18)$$

$$\varepsilon^T(i) = [\varepsilon_i^T(1), \varepsilon_i^T(2), \ldots, \varepsilon_i^T(NY)] \quad (19)$$

where $\varepsilon_i(k)$ is the error at instant i with k steps ahead. The tracking error within the output horizon, as well as

the restrictions on the input within the input horizon, are included in performance index J

$$J = tr\left(\varepsilon^T(i)Q\varepsilon(i) + \Delta U^T(i)R\Delta U(i)\right) \tag{20}$$

where $tr(.)$ denotes the trace of a square matrix; Q and R are symmetric, positive, definite matrices; Q is the tracking-error weighting matrix; and R is the control-effort weighting matrix.

The necessary condition for the optimum, $\partial J/\partial \Delta U = 0$, applied to Eq. (20) and using Eq. (13), yields

$$\Delta U(i) = K(Y_o(i) - \overline{Y}(i)) = K\overline{\varepsilon}(i) \tag{21}$$

where

$$K = (G^T Q G + R)^{-1} G^T Q \tag{22}$$

and $\overline{\varepsilon}(i) = Y_o(i) - \overline{Y}(i)$ is the predicted output error. The resulting control increment $\Delta U(i)$ covers the whole input-horizon NU; for control purposes, however, only the first component (the current control increment) is used. Let k denote the first nu rows of K:

$$k = eK, \quad e = [I_{nu} \;\; 0 \;\; 0 \ldots 0] \tag{23}$$

Then the control increment at instant i is

$$\Delta u(i) = k(Y_o(i) - \overline{Y}(i)) = k\overline{\varepsilon}(i) \tag{24}$$

and the control input is obtained from Eq. (6)

$$u(i) = u(i-1) + \Delta u(i) \tag{25}$$

Combining Eqs. (24), (25), (14), (15), and (16), one obtains the control command at moment i:

$$u(i) = u(i-1) + k\left(Y_o(i) - \overline{Y}(i)\right)$$

$$= u(i-1) + kY_o(i) - kHx(i) - kFU(i-1)$$

and with $u(i-1) = eU(i-1)$, the above equation yields

$$u(i) = kY_o(i) - kHx(i) + (e - kF)U(i-1) \tag{26}$$

Thus, the command $u(i)$ depends on the previous input horizon $U(i-1)$, on the actual state $x(i)$, and on the control command $Y_o(i)$ up to NY steps ahead.

The closed-loop system equations are obtained by combining the plant equation, Eq. (1), with the controller equation, Eq. (26), and by introducing the new state variable $U_o(i)$ such that

$$U_o(i+1) = U(i) \tag{27}$$

In this way, one obtains

$$x(i+1) = (A - BkH)x(i) + B(e - kF)U_o(i) + BkY_o(i)$$

$$U_o(i+1) = -KHx(i) + (I_N - KF)U_o(i) + KY_o(i)$$

$$y(i) = Cx(i) \tag{28}$$

and $N = NU \times nu$. With the new state variable $z^T = [x^T, U_o^T]$, the closed-loop equations are

$$z(i+1) = A_c z(i) + B_c Y_o(i), \quad y(i) = C_c z(i) \tag{29}$$

where

$$A_c = \begin{bmatrix} A - BkH & B(e - kF) \\ -KH & I_N - KFF \end{bmatrix}$$

$$= \begin{bmatrix} (I_n - BK \;\; \mathcal{O}_{NY-1})A & B(e - kF) \\ -KH & I_N - KF \end{bmatrix} \tag{30}$$

$$B_c^T = [Bk \;\; K]^T, \quad C_c = [C \;\; 0] \tag{31}$$

One can see that control command $u(i)$ is now

$$u(i) = kY_o(i) + [-kH \;\; e - kF]z(i) \tag{32}$$

fully recovered from the current state of the system and from the input command.

The block diagram for the closed-loop system, Eqs. (29)–(31), is presented in Fig. 2. The system consists of the plant, the predictor (PRD), the controller (CO),

and the command horizon generator (CHG). The predictor structure is shown in Fig. 3(a) and the command horizon generator in Fig. 3(b). The state-space representation of the command horizon generator is

$$A_{rh} = \begin{bmatrix} 0 & I & 0 & \dots & 0 \\ 0 & 0 & I & \dots & 0 \\ \dots & \dots & \dots & \dots & \dots \\ \dots & \dots & \dots & \dots & \dots \\ 0 & 0 & 0 & \dots & I \\ 0 & 0 & 0 & \dots & 0 \end{bmatrix}, \quad B_{rh} = \begin{bmatrix} 0 \\ 0 \\ \cdot \\ \cdot \\ 0 \\ I \end{bmatrix},$$

$$C_{rh} = \begin{bmatrix} I & 0 & \dots & 0 \\ 0 & I & \dots & 0 \\ \dots & \dots & \dots & \dots \\ \dots & \dots & \dots & \dots \\ 0 & 0 & \dots & I \\ 0 & 0 & \dots & 0 \end{bmatrix}, \quad D_{rh} = \begin{bmatrix} 0 \\ 0 \\ \cdot \\ \cdot \\ 0 \\ I \end{bmatrix} \tag{33}$$

where I is an identity matrix of order ny, and A_{rh} and B_{rh} have $NY - 1$ rows, while C_{rh} and D_{rh} have NY columns.

The weighting matrices R and Q are the tuning parameters of the optimal design (for example, see [2,12]). That means they are to be adjusted until satisfactory results are obtained. Although they are not "active" in the optimal design solution, their choice significantly influences the performance and stability of the system. A general procedure for a reasonable choice of the weighting matrices is not yet known. In this article, a simplified procedure is developed. The weighting matrices obtained from this procedure significantly improve system performance, i.e., tracking error.

A diagonal matrix $R = \rho I$ has been chosen as a control weighting matrix, where $\rho > 0$ is a scalar, and tracking-error weighting matrix Q has the following structure:

$$Q = diag(q, \alpha q, \alpha^2 q, \dots, \alpha^{NY-1} q) \tag{34}$$

The diagonal component $q\alpha^{k-1}q$ is the weight of the error of $\varepsilon_i(k)$, the kth component of $\varepsilon(i)$. The last weight is time dependent; the weight of the output error at the $(i+k)$th time instant is α^{k-1}. The scalar α is called a forgetting factor. The most recent output is given a unit weight, and the future output penalized (in fact, awarded, as will be shown later) exponentially. With this arrangement, the choice of R and Q reduces to the choice of parameters ρ, α, and q, as is illustrated in Section V.B.

There are two sources of system disturbances: measurement noise $v_y(i)$ (or $v_x(i)$ when measuring all state variables) and input disturbances $v_u(i)$ (Fig. 2). The disturbances are included in the closed-loop system model, with the triple (A_c, B_y, C_c) for the output noise and the triple (A_c, B_u, C_c) for the input disturbances, where

$$B_y = \begin{bmatrix} A - BkH \\ -KH \end{bmatrix},$$

$$B_u = \begin{bmatrix} B(e - kF)e_v \\ (I - KF)e_v \end{bmatrix}, \quad e_v = \begin{bmatrix} I_{nu} \\ 0 \end{bmatrix}$$

Their impact on system performance is studied in Section V.D. For high-frequency disturbances, the disturbance-rejection properties of the system significantly improve when the lowpass filter (LPF) is applied as in Fig. 4(a). The plant states related to the command signal are obtained from the plant model (PM), and they are extracted from the measured states. The resulting signal passes through a lowpass filter and is added to the states previously extracted. The filter is shown in Fig. 4(b).

IV. Predictive Estimation

Implementation of the predictive controller depends on the availability of the plant states for measurement. Often, these parameters are not available. An LQ estimator (for example, see [2,13]) that estimates plant state from its output can be considered as a solution to the problem. Its action, however, is too slow for the predictive control system, and the predictive scheme is included in the design of the estimator. Thus, a new estimator with dynamic characteristics comparable to the predictive controller is developed.

The estimate $\hat{x}(i)$ of the plant state $x(i)$ is determined from the input and output horizons as follows. From Eq. (1), one obtains

$$CA^k x(i) = y(i+k) - \sum_{j=1}^{k} CA^{j-1} Bu(i+k-j),$$

$$k = 0, 1, 2, ..., NY$$

or

$$\mathcal{O}_{NY} x(i) = Y_e(i) - G_e U(i) \tag{35}$$

where

$$\mathcal{O}_{NY} = \begin{bmatrix} C \\ H \end{bmatrix}, \quad Y_e(i) = \begin{bmatrix} y(i) \\ Y(i) \end{bmatrix}, \quad G_e = \begin{bmatrix} 0 \\ G \end{bmatrix} \tag{36}$$

and H, G, and Y are given in Eqs. (15), (12), and (7), respectively. Variable Y_e is an augmented output horizon composed of the current output $y(i)$ and the output horizon $Y(i)$. From Eq. (35), the estimate $\hat{x}(i)$ of $x(i)$ is determined such that for a symmetric, positive, weighting matrix Q_e the estimation index

$$J_e = \|H_e x(i) - H_e \hat{x}(i)\|^2_{Q_e} \tag{37}$$

is minimal, obtaining

$$\hat{x}(i) = \mathcal{O}^+_{NY}(Y_e(i) - G_e U(i)) \tag{38}$$

where $\mathcal{O}^+_{NY} = (\mathcal{O}^T_{NY} Q_e \mathcal{O}_{NY})^{-1} \mathcal{O}^T_{NY} Q_e$. Note that the state estimate is determined from input and output horizons, while input and output signals, rather than horizons, are available for estimation. The input horizon is available, however, right after the controller output (Fig. 2). Output horizon $Y(i)$ is not available directly; nevertheless, it can be obtained from the plant model as follows:

$$X(i+1) = AX(i) + BU(i), \quad Y(i) = CX(i) + DU(i) \tag{39}$$

The estimator is shown in Fig. 5(a). Thus, the plant state is estimated from its output and the input horizon. This scheme is similar to the LQ estimation scheme, since it uses the available input and output signals and the plant model to generate the estimate. The block diagram of the predictive control system with the predictive estimator (EST) is shown in Fig. 6.

Unlike the LQ estimator, the predictive estimator does not have filtering properties, since its output $\hat{x}(i)$ is proportional to a noisy signal $y(i)$. This drawback can be removed as follows. Given the plant model output $y_n(i)$ the output error $\varepsilon_y(i) = y(i) - y_n(i)$ is filtered by a proper filter, obtaining the filtered error $\varepsilon_{yf}(i)$. In most cases, the output error is a high-frequency noise; hence, a lowpass filter is applied. The filtered output is obtained by adding a filtered error to the nominal output $y_f(i) = y_n(i) + \varepsilon_{yf}(i)$. In this way, most of the noise power is removed from the output signal, while the basic properties of the signal remain untouched. The estimator with a filter is shown in Fig. 5(b). The filter action will be illustrated in the next section.

V. Predictive Control and Estimation for the DSS 14 Antenna

Performances of the predictive controller and estimator are checked through tracking simulations of the DSS 14 National Aeronautics and Space Administration (NASA)/ Jet Propulsion Laboratory (JPL) 70-meter DSN antennas. The existing control scheme for the DSN 70-m antennas [14] is based on an LQ regulator design with the integral action as presented in [15–20]. The LQ control system is shown in Fig. 7, in which the plant output is augmented by the addition of the output integrals in order to ensure the zero mean value of the constant-rate tracking error. The LQ controller is designed for this augmented plant with a constant tracking command. This assumption can be a significant source of tracking error. A controller designed for the constant tracking command can result in insufficient antenna performance, especially for relatively fast commands or varying rate commands. In this section, the performance of the predictive controller is compared with that of the LQ controller in the tracking environment.

A. Plant Model

The state-space model of the DSS 14 antenna [14] is a four-state model with position rate u as an input and position rate y as an output. Its discrete-time representation (A_d, B_d, C_d), with the sampling period $\Delta t = 0.05$ sec, is obtained from the continuous-time representation in [2]:

$$A_d = \begin{bmatrix} 0.0468 & 0 & 0 & 0 \\ 0 & 0.5443 & 0.3474 & 0 \\ 0 & -0.3474 & 0.5443 & 0 \\ 0 & 0 & 0 & 0.8872 \end{bmatrix},$$

$$B_d = \begin{bmatrix} 0.0113 \\ 0.0025 \\ 0.0399 \\ 0.0538 \end{bmatrix}, \quad C_d = [0.7239 \quad 9.2260 \quad 0 \quad 1.1421]$$

The system (A_d, B_d, C_d) is augmented. As a result, its output consists of the position rate, the angular position, and the integral of the position. The augmented system is shown in Fig. 8. Denoting x_d the state of the system (A_d, B_d, C_d), and x_{po} and x_{ipo} the position and the integral of the position, respectively, one obtains from Fig. 8

$$x_{ipo}(i+1) = x_{ipo}(i) + \Delta t x_{po}(i)$$

$$x_{po}(i+1) = x_{po}(i) + \Delta t C_d x_d(i)$$

$$x_d(i+1) = A_d x_d(i) + B_d u(i)$$

With the plant-state variable $x^T = [x_{ipo}, x_{po}, x_d^T]$, the triple (A, B, C) is the resulting plant-state space representation

$$A = \begin{bmatrix} 1 & \Delta t & 0 \\ 0 & 1 & \Delta t C_d \\ 0 & 0 & A_d \end{bmatrix}, \quad B = \begin{bmatrix} 0 \\ 0 \\ B_d \end{bmatrix}, \quad C = \begin{bmatrix} 1 & 0 & 0 \\ 0 & 1 & 0 \\ 0 & 0 & C_d \end{bmatrix}$$

used in simulations presented below.

B. Weighting Matrices and Input and Output Horizons

For simulation purposes, a piecewise-linear profile of the position command is chosen, with linear increase followed by linear decrease and the final constant value (Fig. 9). The command rate is 4 mdeg/sec, which is a typical sidereal tracking rate. The shape of the command is more dramatic than the real tracking command, but it has been chosen to emphasize the tracking possibilities of the predictive controller. A more realistic tracking command will be used later in this article.

In order to perform a series of simulations, weighting matrices R and Q are chosen such that the output error is small while the control effort is maintained within reasonable limits. For diagonal-control weighting matrix $R = \rho I$, parameter $\rho = 0.01$ is chosen. Tracking-error weighting matrix Q is as in Eq. (34). Component q is in the form $q = \text{diag}(q_i, q_p, q_r)$. It represents the weight of the integral, position, and rate components of the output. The following choices of weight are recommended from a series of simulations tracking the command as in Fig. 9: for the integral-of-the-position signal, $q_i = 10$; for the position signal, $q_p = 1$; and for the rate signal, $q_r = 0.1$. Coefficient α^{k-1} in the weighting matrix is the weight of the kth error component in the output horizon. Simulations have been performed in order to determine the value of parameter α. The plot of the Euclidean norm of tracking error $\|y - y_o\|_2$ versus α is shown in Fig. 10 both for different lengths of output horizon and for lengths of input and reference horizon equal to lengths of output horizon. The plot shows the minimal tracking error obtained for $\alpha = 6.2$ and $NY = NU = NR = 6$. For $NR = NU = NY$, Fig. 11 plots the values of α for which the tracking error is minimal. The figure shows that, for horizons that are long enough, the forgetting factor is close to 1. Thus, in this case, the time weighting does not significantly improve the tracking error. However, for short horizons, the proper choice of forgetting factor is a critical factor that minimizes the error dramatically. In prediction, the forgetting factor is greater than one (thus, "reminding factor" could be an adequate name for it). This is in contrast to the forgetting factor value in estimation procedures such as in [12], where the factor is smaller than one. This difference occurs due to opposite time directions; in estimation, the past values of signal are weighted, while in prediction the future values of signal are processed.

From simulations, the impact of the length of input-reference horizon NR and output horizon NY on the tracking error is determined. The results are plotted in Fig. 12. One can see that for $NR \geq n/2$ and $NY \geq 2n$ (where $n = 6$ is the number of plant-state variables), the performance error is close to the minimal one.

C. Antenna Performance

The performance of the DSS 14 antenna with the tracking command as shown in Fig. 9 has been evaluated for the parameters recommended above. The following parameters for the predictive controller were chosen: $NR = NU = NY = n = 6$ and weighting matrices with $\rho = 0.01$, $q = \text{diag}(10, 1, 0.1)$, and $\alpha = 6.2$. The reference signal and the position of the antenna with the predictive controller for $\alpha = 6.2$, for $\alpha = 1$, and for the antenna with the LQ controller are shown in Fig. 9. The prediction errors and control input for the above three cases ($\alpha = 6.2$, $\alpha = 1$, and LQ controller) are shown in Figs. 13 and 14. The figures show better performance by the predictive controllers than by the proposed LQ controller with comparable control effort. Also, predictive-controller performance with time-weighted output error ($\alpha > 1$) is better than predictive-controller performance without time weighting ($\alpha = 1$).

The minimum of tracking error for output horizon $NY = 4$ is obtained for $\alpha = 6.4$. These two parameters are used in further simulations, since it is reasonable to have the length of the output horizon as small as possible; the dimension of the controller as well as the complexity of the system depend on NY. The step-response and frequency-response plots of the closed-loop system with a predictive controller and an LQ controller are compared in Figs. 15 and 16. Figure 15 shows that the settling time and overshoot for the system with the predictive controller, with $NY = NU = NR = 4$ and $\alpha = 6.4$, are significantly reduced from the system with the LQ controller. Similarly, from Fig. 16, one can see the tracking performance is improved; the magnitude of the closed-loop transfer function is equal to 1 over a wider bandwidth. Also, roll-off rate is improved for the system with a predictive controller (with $NY = NU = NR = 4$ and $\alpha = 6.4$, as well as with $NY = NU = NR = 6$ and $\alpha = 5$) when compared to the system with an LQ controller.

The piecewise constant-rate command, as well as the unit step command, are dramatic scenarios for the DSS 14

antenna and have been introduced in order to present dynamic possibilities of the predictive control. In order to meet the typical working requirements for the antenna, the raised-cosine command is introduced, as in Fig. 17 (solid line). This kind of command is close to the real elevation or azimuth trajectory of the antenna (conscan-like tracking). The plot of the output of the predictive control system overlaps the plot of the command, while the output of the LQ control system is plotted by a dashed line (Fig. 17). The tracking error, the difference between the output and the command, is plotted in Fig. 18(a) for the LQ control system and in Fig. 18(b) for the predictive control system. For the LQ control system, the error is on the order of 10^{-4}, while the error for the predictive control system is on the order of 10^{-7}. In both cases, however, the control effort is almost the same (Fig. 19).

D. Robustness and Disturbance Suppression

The robustness of the closed-loop system to the plant-parameter variations is checked as follows. The plant poles are randomly perturbed within 20 percent margin, and the error in the step-command tracking is simulated for 500 random samples. The results of the simulations are presented in Fig. 20. On the average, tracking error has changed about 5 percent in comparison with the nominal plant error, and the maximal tracking error is 66 percent larger than the nominal plant error. The step and frequency responses of the closed-loop system for the nominal plant and for the plant model deviated 20 percent from the nominal, as is shown in Figs. 21 and 22. Both plots show good performance and robustness of the system.

Two sources of disturbances of the antenna are studied: the input disturbances and output disturbances (measurement noise). The input-disturbance transfer functions (from v_u to y) and output-disturbance transfer functions (from v_x to y) are shown in Fig. 23, the latter one for both position- and rate-measurement noise. One can see from Fig. 23 that the input disturbances are significantly suppressed, while the position-measurement noise is amplified over certain frequency ranges.

The nature of the antenna disturbances is not satisfactorily known, and here their general properties are outlined. Input disturbances, such as wind or thermal forces, are low-frequency signals. Measurement noise, on the other hand, is a high-frequency signal (high in comparison to the antenna fundamental frequency, which is less than 1 Hz). Therefore, for testing purposes, white-noise input disturbances and high-frequency measurement noise with frequency components over 3 IIz are applied. The system response due to different signal-to-noise (S/N) ratios is simulated. The results are compared in Fig. 24, where good disturbance-suppression properties of the system are observed. The impact of the input noise is much smaller than that of measurement noise. This feature can be explained with the lowpass-filtering property of the plant; the noise is filtered before entering the predictor. The tracking error and plant input for input noise with S/N ratio = 10 and for measurement noise with S/N ratio = 100 are shown in Figs. 25 and 26. The effect of the measurement noise is reduced by applying a filter, as in Fig. 4. The transfer-function plots from the output disturbances to the system output for the system with the filter are shown in Fig. 27. The tracking error due to measurement noise is reduced significantly, even for white noise (Fig. 28).

E. Predictive Estimator

Predictive-estimator performance is compared to the performance of the LQ estimator. The plant model (A_d, B_d, C_d) has been used for simulations, with unit-step input and zero-initial conditions. For estimation purposes, the initial conditions have been changed to $[0.1\ 0.1\ 0.1\ 0.1]^T$. The estimation results are shown in Fig. 29. The LQ estimator needs approximately 2 seconds to reach an acceptable estimation error, while the predictive estimator determines the states in virtually no time. In the case of noisy output, with S/N ratio = 100, one obtains estimation errors for the LQ and predictive estimators (with and without filter) as in Fig. 30. The unfiltered predictive estimate in Fig. 30(b) would make the estimator useless for prediction purposes. However, these errors are reduced by a filter, as in Fig. 30(c). The maximum error of the predictive estimator with a filter is much smaller than the residual error of the LQ estimator even after 4 seconds in action. Finally, simulations indicate that the identity-weighting matrix ($Q_e = I$) is the optimal choice for estimation purposes.

VI. Conclusions

In this article, a modified state-space predictive controller is introduced, and a predictive estimator is presented to complement the design of a predictive-control law. This approach has been used for the design of the tracking controllers of the NASA/JPL 70-m antennas. Several tracking scenarios have been introduced (step input, constant-rate rise and fall, raised-cosine trajectory) to test the tracking behavior of the predictive controller. Significant improvement of performance for presented scenarios has been observed. It has been shown that the time for the predictive estimator to reach an acceptable level of estimation error is much smaller than that for the LQ estimator. Also, a wider bandwidth and improved roll-off

rate is obtained for the predictive closed-loop system in comparison with the LQ regulator system. The predictive control system is robust to the plant-parameter variations. Shifts of plant poles of 20 percent of their nominal values keep the tracking performance good; the tracking error is on the same order as for a nominal plant. Disturbance-suppression properties of a predictive control system also have been simulated and found to be good for input disturbances and measurement noise if the measurement-noise spectrum is higher than the plant-fundamental frequency. The system disturbance-suppression properties can be enhanced if the disturbance filter is included in the system.

Acknowledgments

The author wishes to thank Ben Parvin for recognizing the importance of predictive control in DSN antenna design and for introducing technical aspects of DSN antenna controls, and Leon Alvarez for discussions about the DSS 14 antenna model.

References

[1] P. Albertos and R. Ortega, "On Generalized Predictive Control: Two Alternative Formulations," *Automatica*, vol. 25, no. 5, pp. 753–755, October 1989.

[2] B. D. O. Anderson and J. B. Moore, *Optimal Control*, Englewood Cliffs, New Jersey: Prentice-Hall, 1990.

[3] K. J. Astrom and B. Wittenmark, *Adaptive Control*, Reading, Pennsylvania: Addison-Wesley, 1989.

[4] D. W. Clarke and C. Mohtadi, "Properties of Generalized Predictive Control," *Automatica*, vol. 25, no. 6, pp. 859–875, December 1989.

[5] D. W. Clarke, C. Mohtadi, and P. S. Tuffs, "Generalized Predictive Control, Part I and II," *Automatica*, vol. 23, no. 2, pp. 137–160, April 1987.

[6] G. C. Goodwin and K. S. Sin, *Adaptive Filtering Prediction and Control*, Englewood Cliffs, New Jersey: Prentice-Hall, 1984.

[7] H. Kwakernaak and R. Sivan, *Linear Optimal Control Systems*, New York: Wiley, 1972.

[8] F. L. Lewis, *Optimal Control*, New York: Wiley–Interscience, 1986.

[9] R. Ortega and G. S. Galindo, "Globally Convergent Multistep Receding Horizon Adaptive Controller," *Int. J. Control*, vol. 49, no. 5, pp. 1655–1664, May 1989.

[10] J. G. Reid, D. E. Chaffin, and J. T. Silverthorn, "Output Predictive Algorithmic Control: Precision Tracking with Application to Terrain Following," *J. Guidance, Control, and Dynamics*, vol. 4, no. 5, pp. 502–509, October 1981.

[11] Y. Xi, "New Design Method for Discrete-Time Multi-Variable Predictive Controllers," *Int. J. Control*, vol. 49, no. 1, pp. 45–56, January 1989.

[12] J. M. Maciejowski, *Multivariable Feedback Design*, Wokingham, England: Addison-Wesley, 1989.

[13] F. L. Lewis, *Optimal Estimation: With an Introduction to Stochastic Control Theory*, New York: Wiley–Interscience, 1986.

[14] L. S. Alvarez and J. Nickerson, "Application of Optimal Control Theory to the Design of the NASA/JPL 70-Meter Antenna Axis Servos," *TDA Progress Report 42-97*, vol. January–March 1989, Jet Propulsion Laboratory, Pasadena, California, pp. 112–126, May 15, 1989.

[15] M. Athans, "On the Design of PID Controllers Using Optimal Linear Regulator Theory," *Automatica*, vol. 7, no. 6, pp. 643–647, December 1971.

[16] S. Fukata, A. Mohri, and M. Takata, "On the Determination of the Optimal Feedback Gains for Multivariable Linear Systems Incorporating Integral Action," *Int. J. Control*, vol. 31, no. 6, pp. 1027–1040, June 1980.

[17] C. D. Johnson, "Optimal Control of the Linear Regulator with Constant Disturbances," *IEEE Trans. Automatic Control*, vol. 13, no. 4, pp. 416–421, August 1968.

[18] B. Porter, "Optimal Control of Multivariable Linear Systems Incorporating Integral Feedback," *Electronics Letters*, vol. 7, no. 8, pp. 170–172, April 1971.

[19] T. Yahagi, "Optimal Output Feedback Control in the Presence of Step Disturbances," *Int. J. Control*, vol. 26, no. 5, pp. 753–762, November 1977.

[20] P. C. Young and J. C. Willems, "An Approach to the Linear Multivariable Servomechanism Problem," *Int. J. Control*, vol. 15, no. 5, pp. 961–979, February 1972.

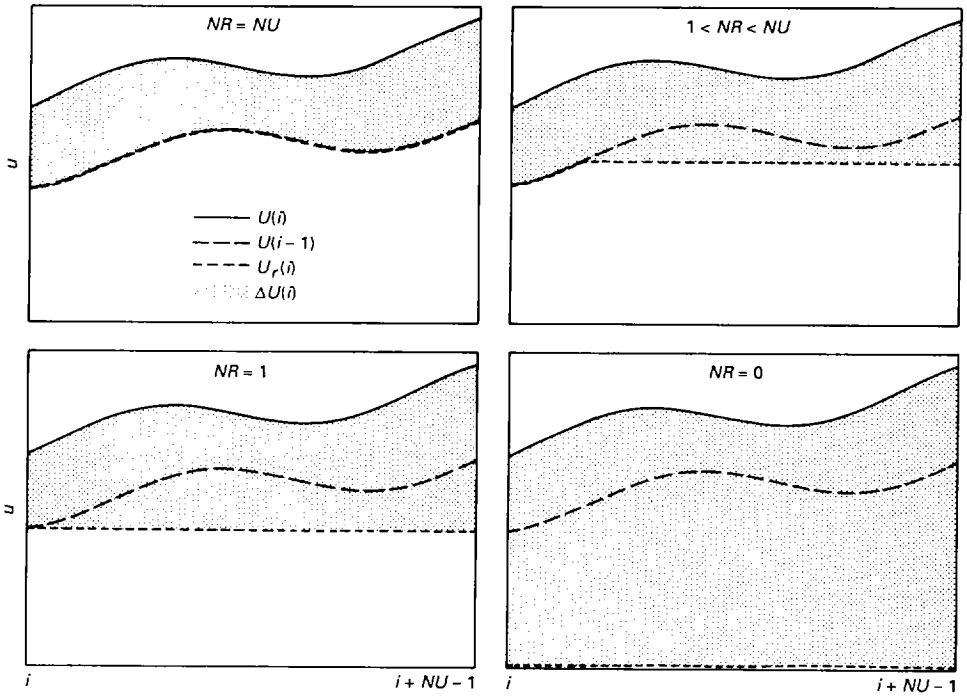

Fig. 1. Input horizons.

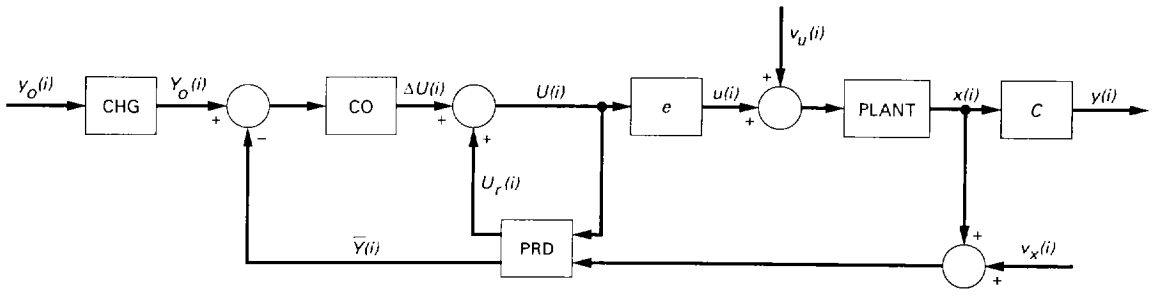

Fig. 2. The predictive control system.

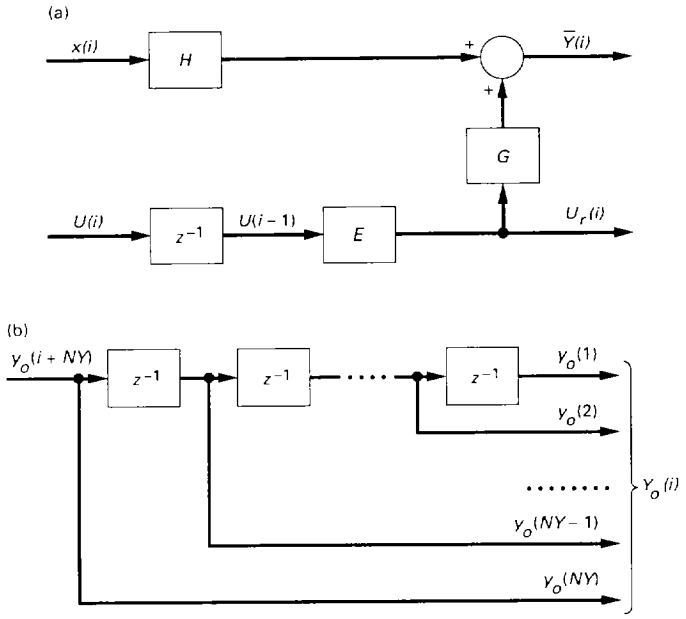

Fig. 3. Block diagrams of (a) the predictor, and (b) the command horizon generator.

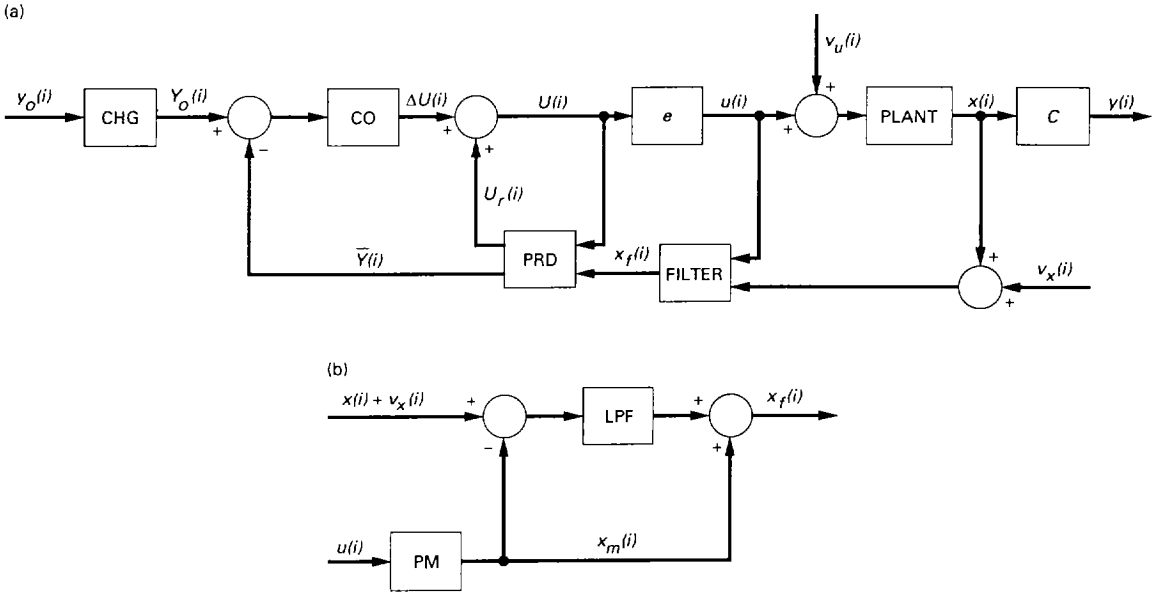

Fig. 4. Block diagrams of (a) the predictive control system with a measurement noise filter, and (b) the measurement noise filter.

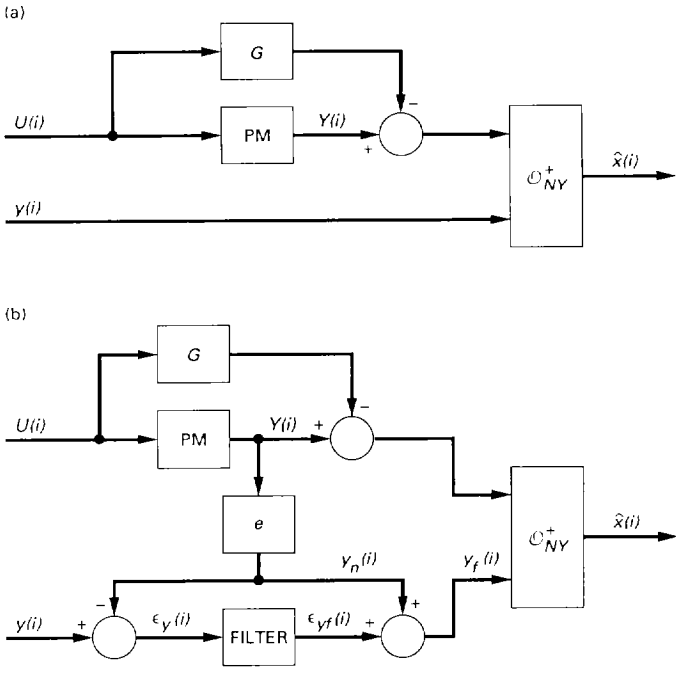

Fig. 5. The predictive estimator: (a) without measurement noise filter, and (b) with measurement noise filter.

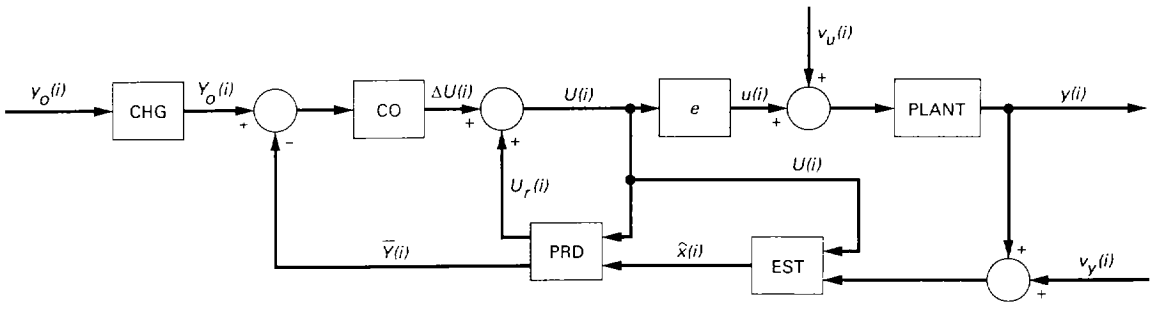

Fig. 6. The predictive control and estimation system.

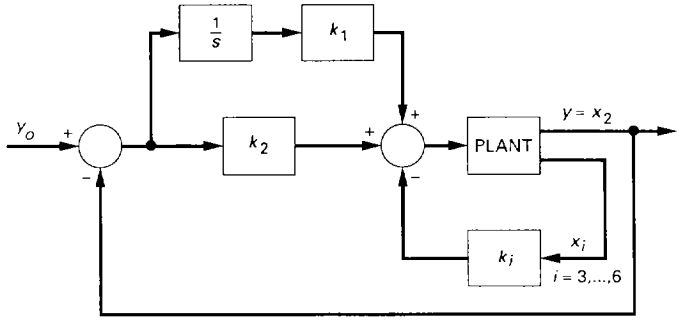

Fig. 7. The LQ control system for the DSS 14 antenna.

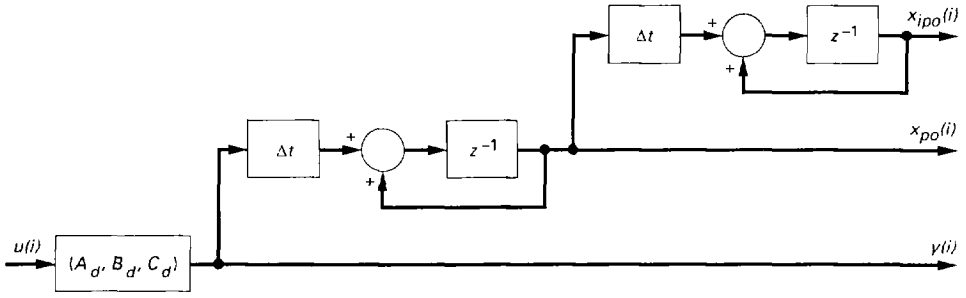

Fig. 8. The augmented model of the DSS 14 antenna.

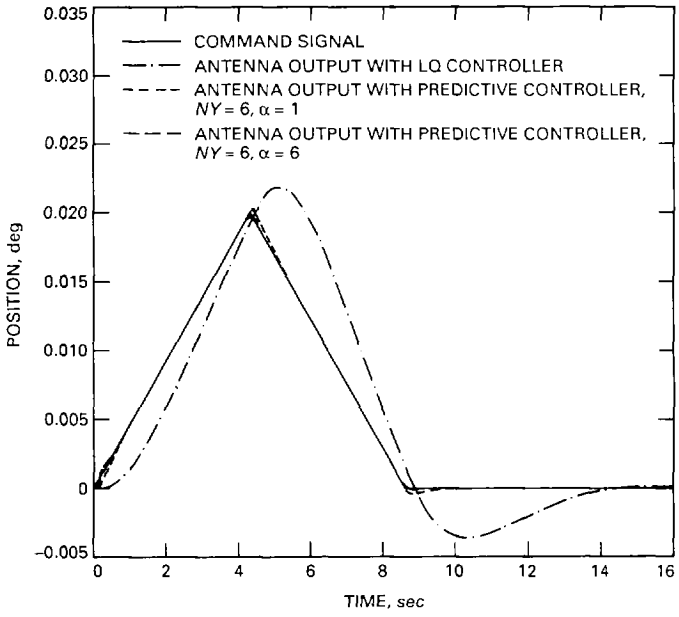

Fig. 9. The command signal and antenna output.

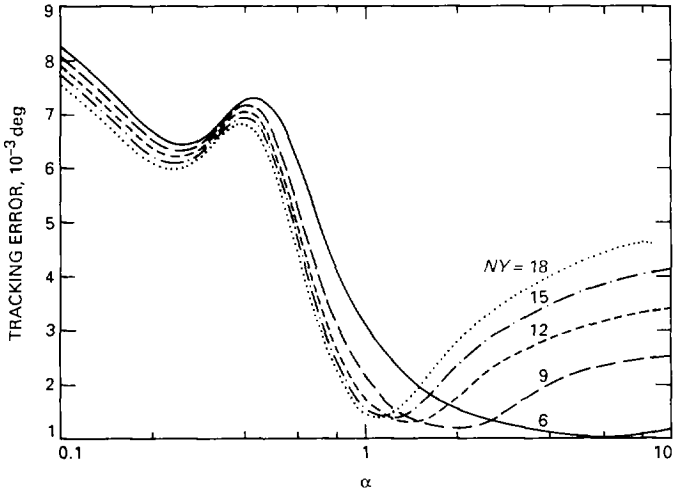

Fig. 10. *Tracking error versus forgetting factor* α *for different lengths of output horizon NY.*

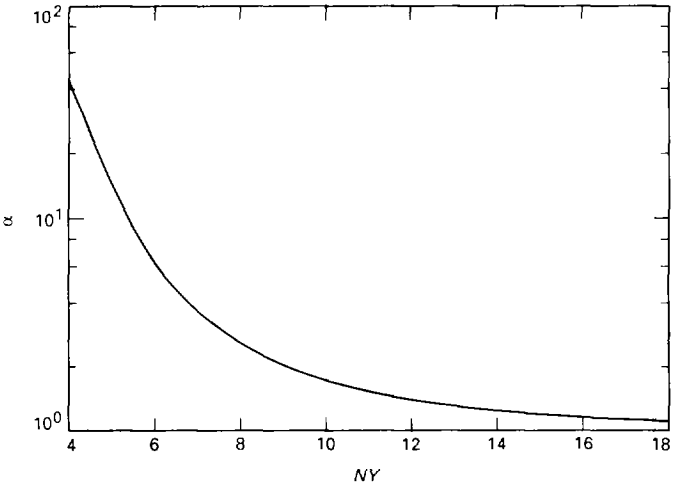

Fig. 11. Forgetting factor α, for which the minimal tracking error is achieved versus length of output horizon *NY*.

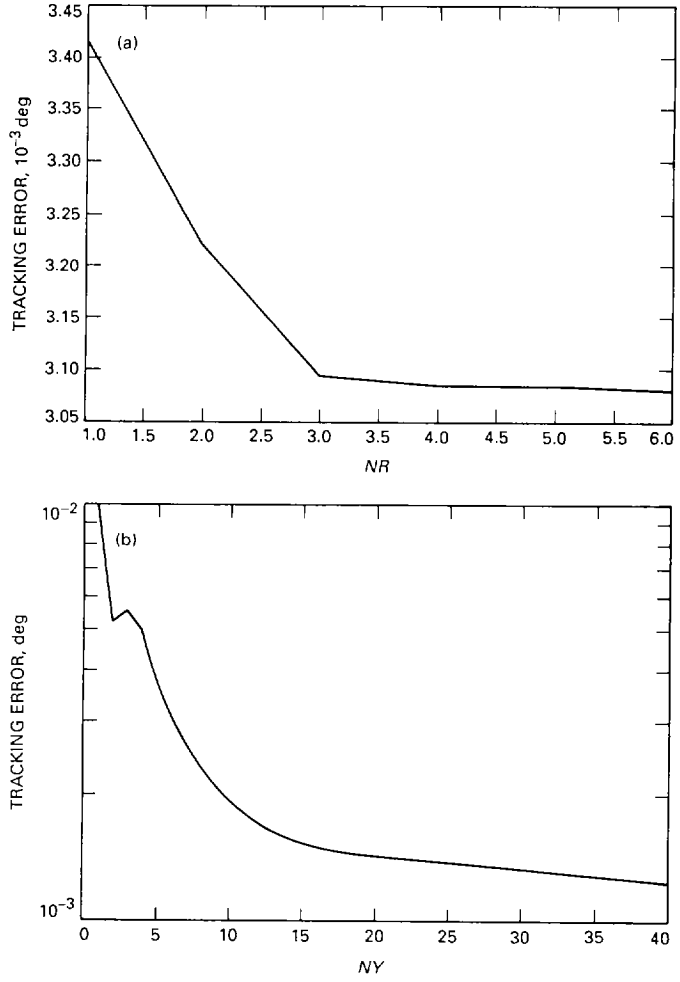

Fig. 12. Tracking error versus: (a) length of reference horizon *NR*, and (b) length of output horizon *NY*.

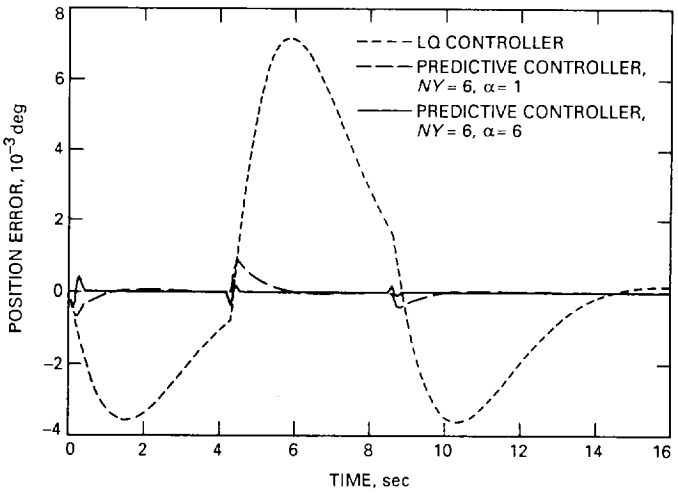

Fig. 13. Tracking error.

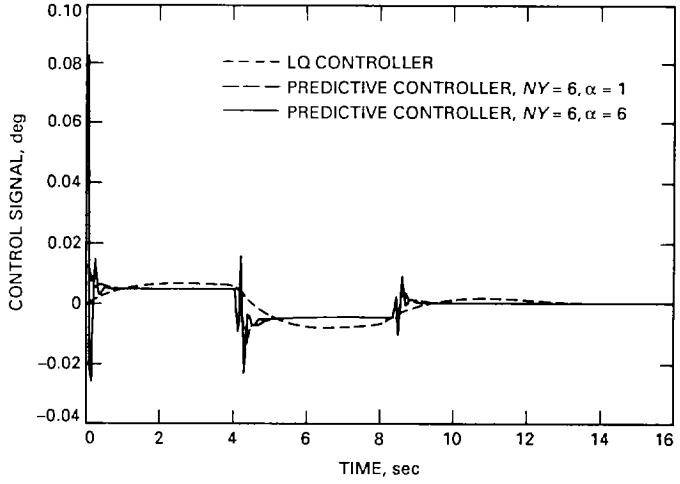

Fig. 14. Antenna control input.

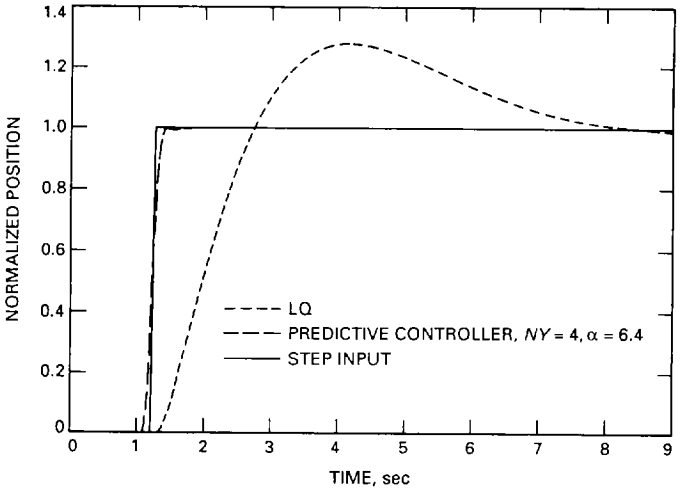

Fig. 15. Closed-loop system step response.

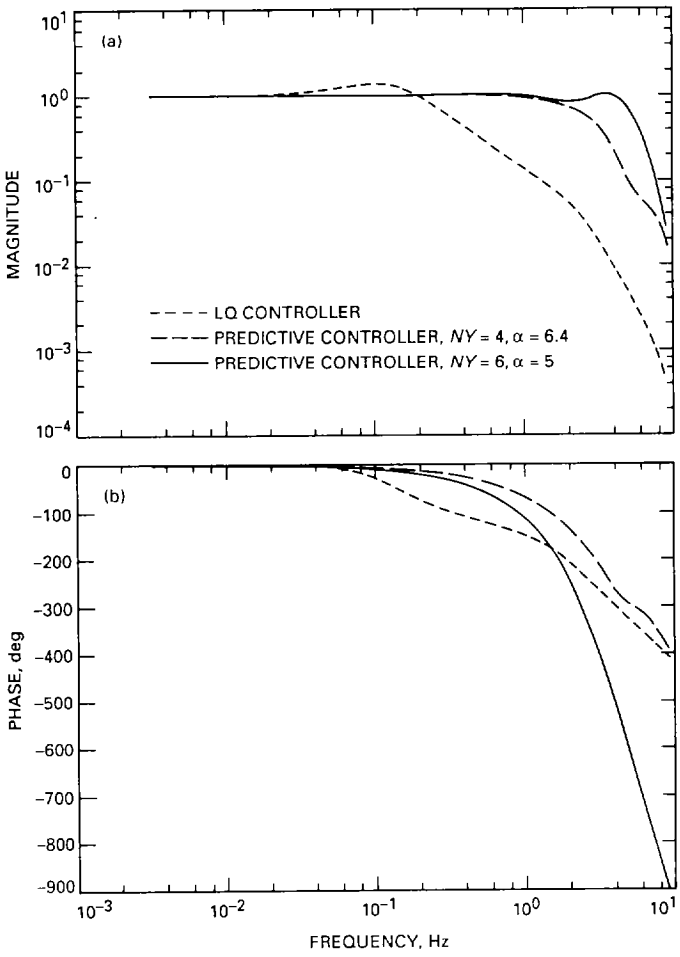

Fig. 16. Closed-loop system frequency response: (a) magnitude, and (b) phase.

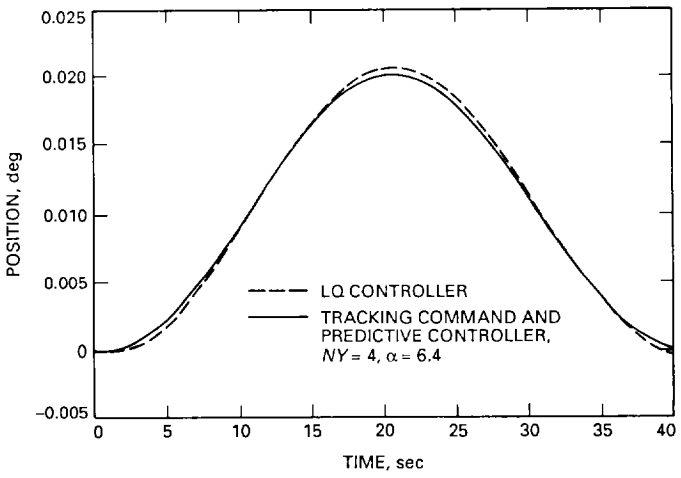

Fig. 17. Closed-loop system tracking performance.

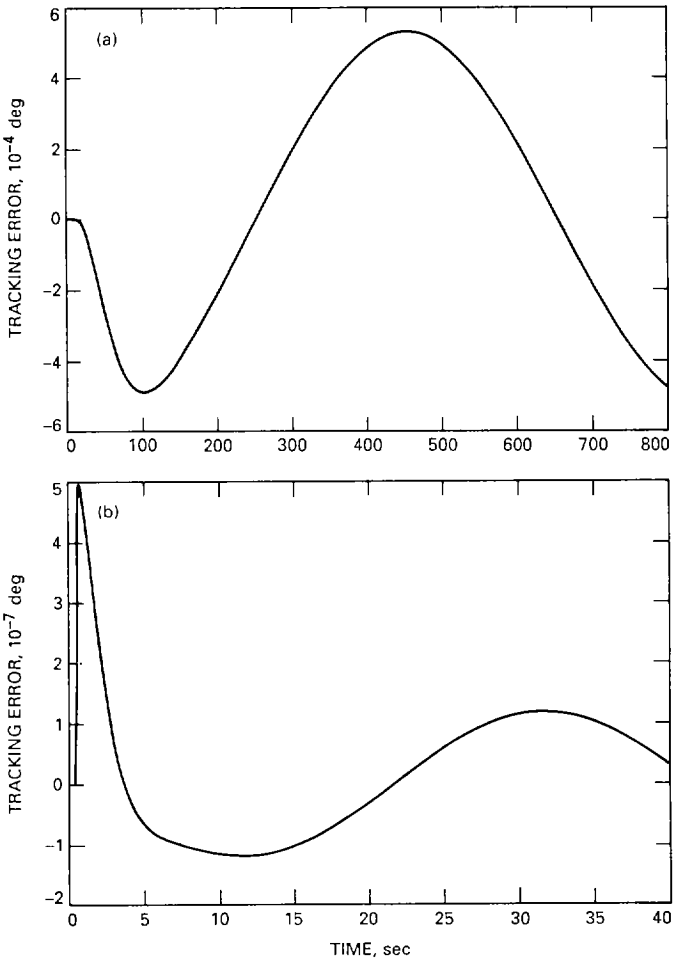

Fig. 18. Tracking error: (a) the LQ regulator system, and (b) the predictive system with $NY = 4$, $\alpha = 6.4$.

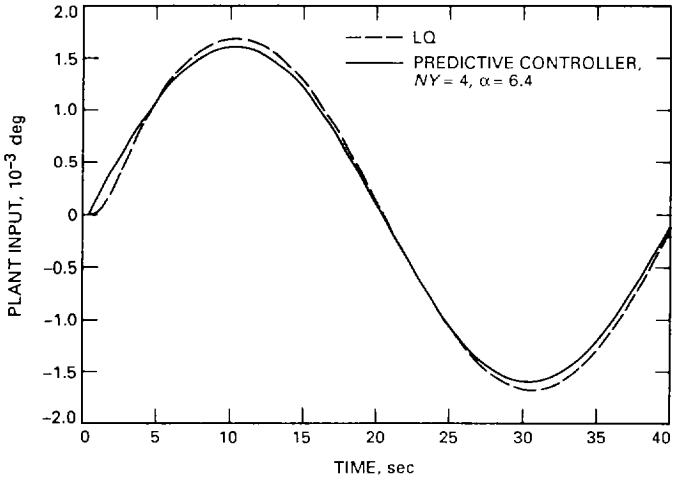

Fig. 19. Antenna input.

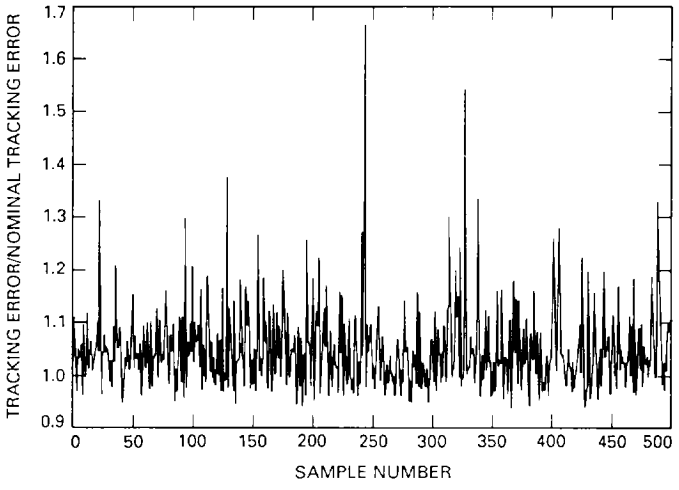

Fig. 20. Tracking-error ratio of the 20-percent randomly deviated model to the nominal model.

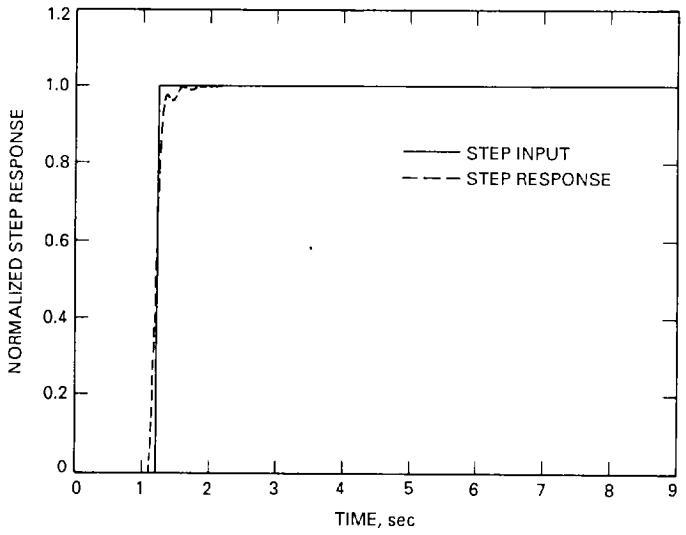

Fig. 21. Closed-loop step response with the 20-percent-deviated model.

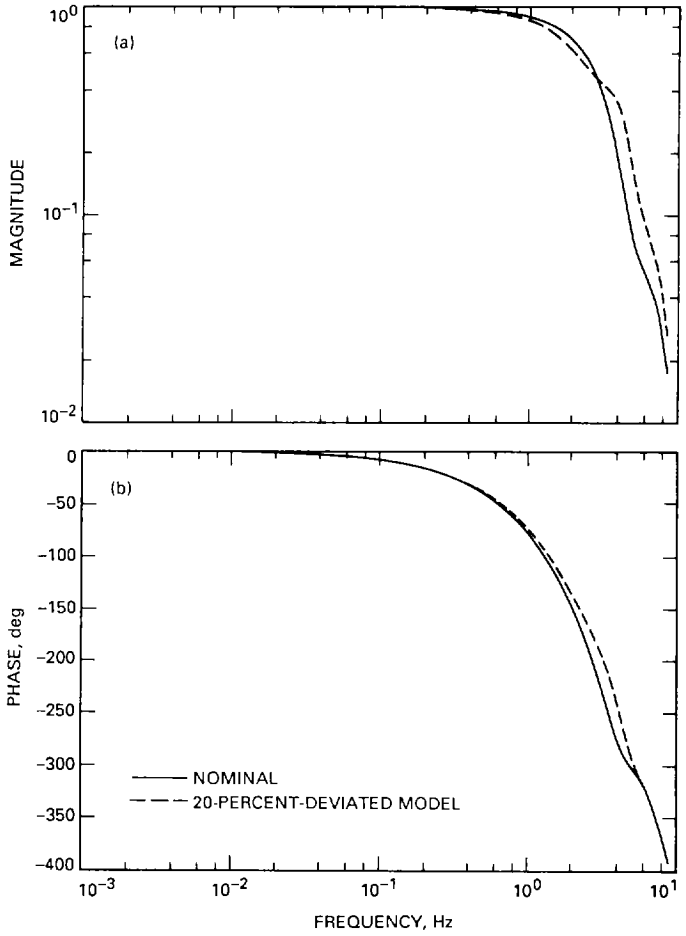

Fig. 22. Closed-loop frequency response: (a) magnitude, and (b) phase.

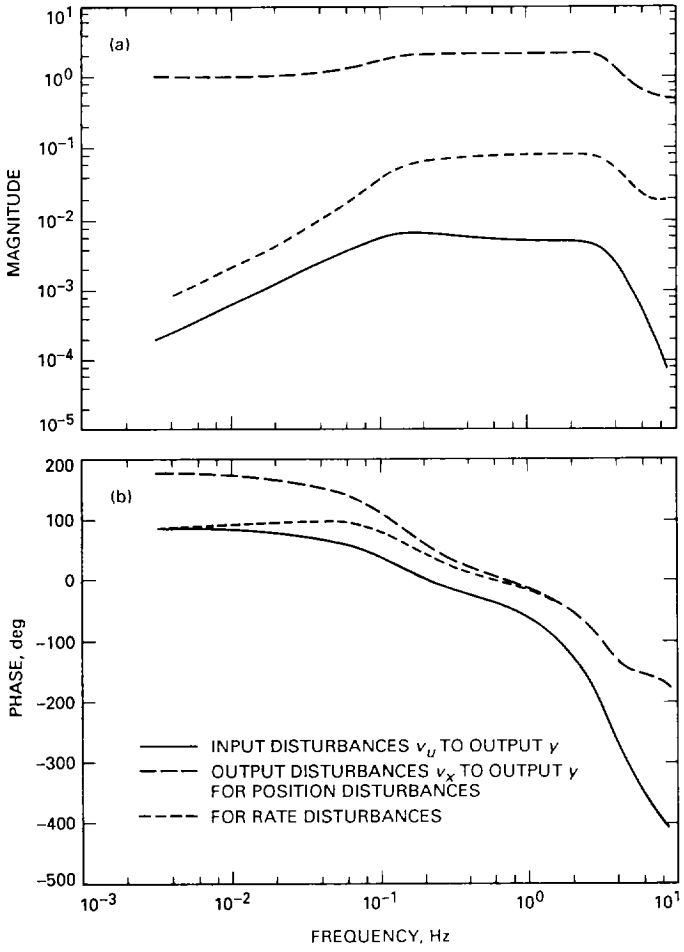

Fig. 23. Transfer functions: (a) magnitude, and (b) phase.

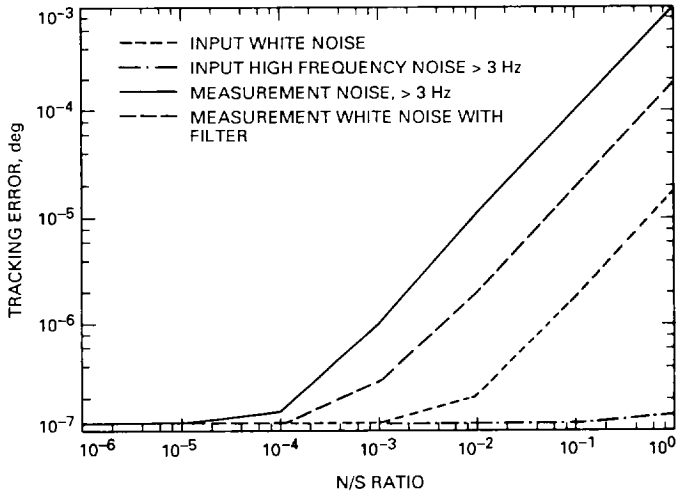

Fig. 24. Tracking errors due to input disturbances.

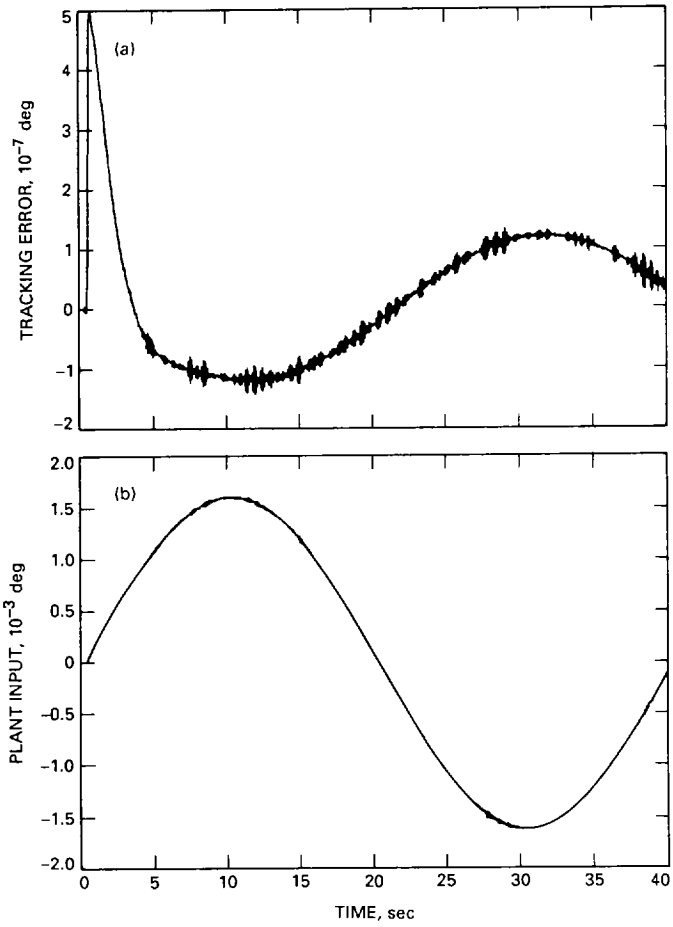

Fig. 25. White noise input disturbances with noise-to-signal ratio = 0.1: (a) tracking error, and (b) antenna input.

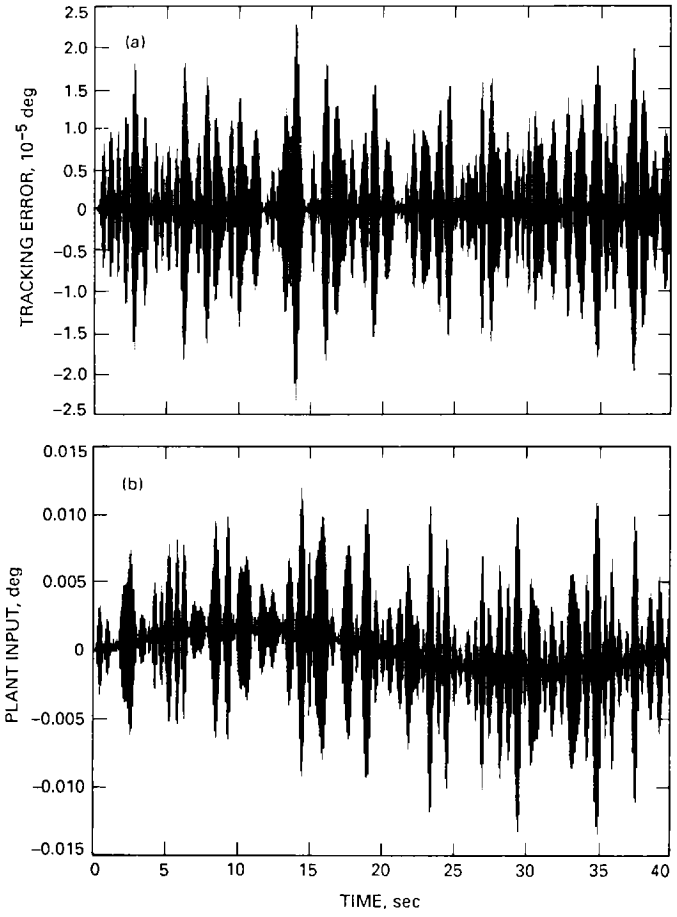

Fig. 26. High-frequency measurement noise with noise-to-signal ratio = 0.01: (a) tracking error, and (b) antenna input.

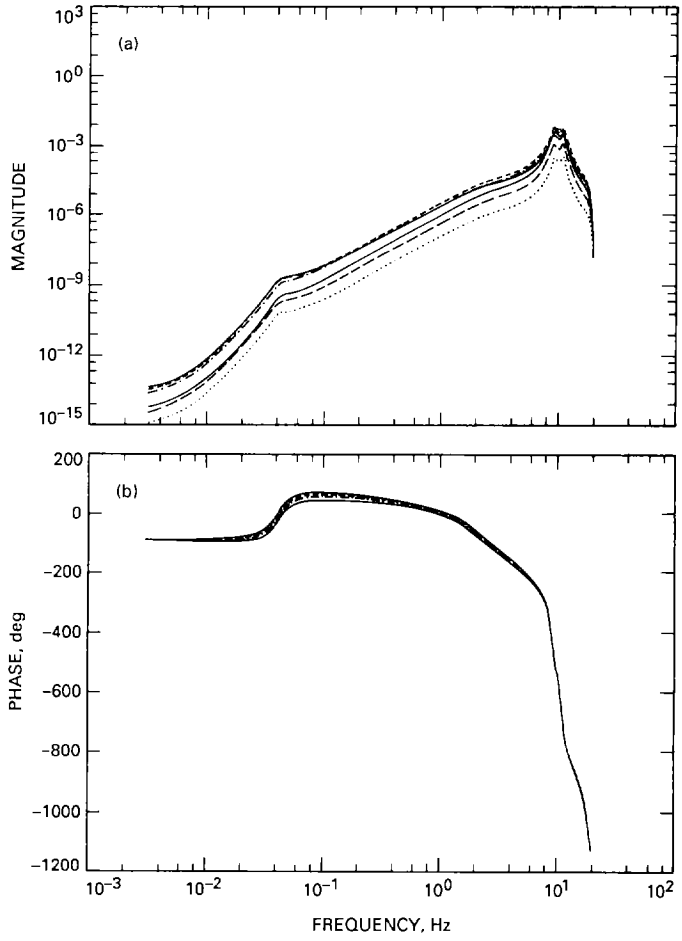

Fig. 27. Transfer functions from output noise v_x (six states) to output y for a system with a noise filter: (a) magnitude, and (b) phase.

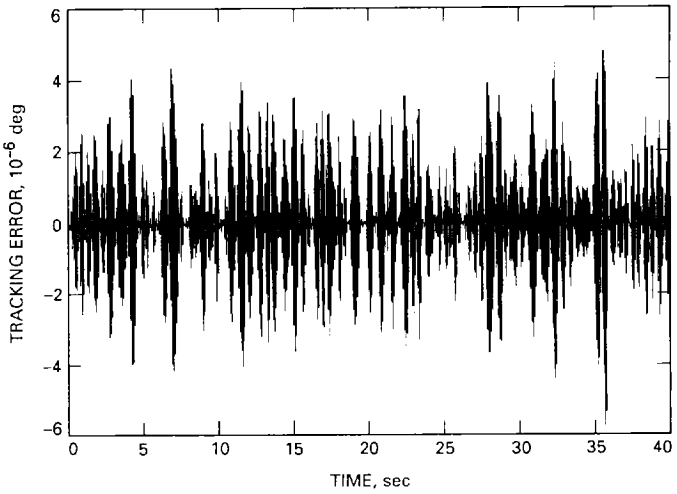

Fig. 28. Tracking error for white-noise output disturbances for a system with a noise filter.

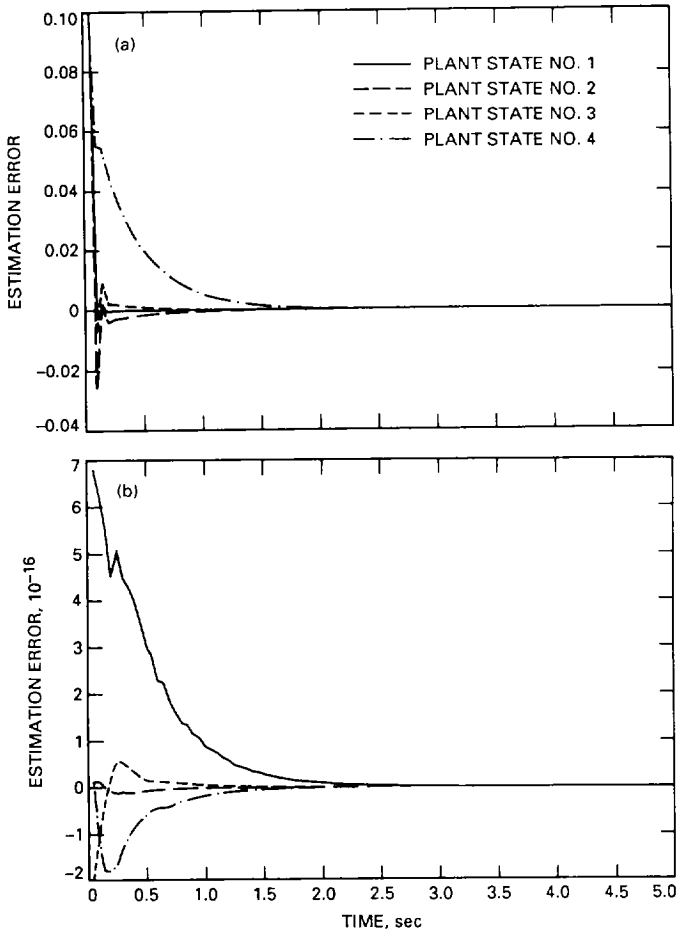

Fig. 29. Estimation error: (a) LQ estimator, and (b) predictive estimator.

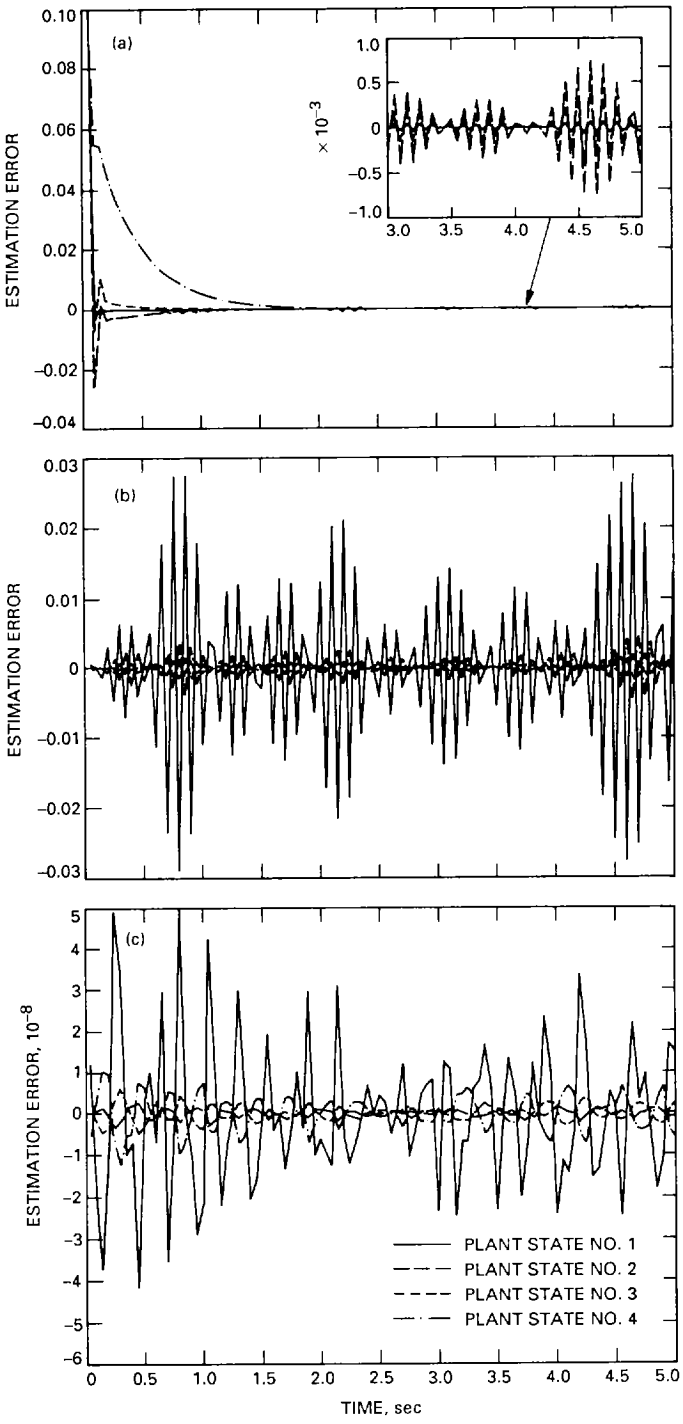

Fig. 30. Estimation error in the presence of measurement noise: (a) LQ estimator; (b) predictive estimator; and (c) predictive estimator with filter.